Tuning the spin signal from a highly symmetric unpolarized electronic state

H. Wortelen,[1,*] H. Mirhosseini,[2,†] K. Miyamoto,[1] A. B. Schmidt,[1] J. Henk,[3] and M. Donath[1]

[1]*Physikalisches Institut, Westfälische Wilhelms-Universität Münster, Wilhelm-Klemm-Straße 10, 48149 Münster, Germany*
[2]*Max-Planck-Institut für Mikrostrukturphysik, Weinberg 2, 06120 Halle, Germany*
[3]*Institut für Physik, Martin-Luther-Universität Halle-Wittenberg, Von-Seckendorff-Platz 1, 06120 Halle, Germany*

A remarkably large spin signal is observed on nonmagnetic W(110) for a highly symmetric unoccupied state with no intrinsic spin polarization. The magnitude and, more importantly, the sign of this spin signal, measured by spin- and angle-resolved inverse photoemission for normal electron incidence, can be tuned in a user-defined manner by variation of the photon-detection angle and/or by rotating the spin-polarization direction of the incident electrons. Using calculations of the orbitally decomposed spectral densities, this effect is traced back to a mixing of different symmetries within the respective state. This explanation is underlined by the behavior of a second electronic state of pure symmetry, which does not show such a spin signal. In general, the spin signals of electronic states are not only influenced by their intrinsic spin polarization but also by the choice of symmetry-breaking experimental parameters in combination with the particular orbital characters of the states under investigation. The latter permits one to tune the spin signal in magnitude and sign.

Spin- and angle-resolved photoemission (PE) as well as inverse photoemission (IPE) provide us with detailed information about spin-orbit-influenced electronic states [1–5]. Despite the undoubted wealth of experimental results, the information content with respect to the spin polarization is still under debate [6,7]. Recently, spin- and angle-resolved PE experiments on the topological nontrivial surface state of Bi_2Se_3 suggested additional spin-polarization effects on top of the intrinsic spin polarization. The measured spin polarization of photoelectrons excited from the surface state could even be manipulated by the polarization of the incident light [8,9]. Furthermore, spin- and angle-resolved IPE from the paradigmatic Rashba system Bi/Ag(111) showed that the measured spin information does not always reflect the intrinsic spin texture of the surface states. For states with mixed orbital symmetries, the measured spin information may be ambiguous and has to be taken with skepticism [10]. The effects described so far are reported for surfaces with threefold rotational symmetry (point group C_{3v}).

Beyond that, it was shown that spin-polarized photoelectrons, excited by unpolarized light, are emitted from unpolarized bulk-derived electronic states even in normal-emission geometry from Pt(110), Pt(100), Pt(111), and Au(111) [6,11–13]. In these experiments, the observed spin features of photoelectrons were found to be strongly influenced by the crystal symmetry. Similarly, a recently described Dirac-like surface state on W(110) shows spin polarization even for normal photoelectron emission, excited by unpolarized light [14,15]. Besides, W(110) is a prototype system for studying spin-orbit coupling effects with spin-resolved photoemission techniques, since it also hosts Rashba-type bands, spin split for off-normal electron emission [16].

Considering the above, the appearance of spin polarization in (I)PE may be regarded as usual and not surprising.

This raises the question on specific features of the involved electronic states which produce or do not produce large spin signals in (I)PE and how they can be tuned. To answer this question, a well-understood surface system, such as W(110), lends itself to such an investigation.

In this paper, we report on a joint experimental and theoretical study. We show that W(110) hosts simultaneously electronic states which produce a vanishing and a large spin signal. Detailed spin-resolved IPE experiments are presented and then explained by model calculations as well as *ab initio* electronic-structure calculations, allowing one to pinpoint the origin of the effects.

We choose an experimental situation with high symmetry: (i) normal electron incidence on the W(110) surface, (ii) spin-polarization directions within mirror planes of the surface, and (iii) detection of unpolarized light. Importantly, we detect the emitted photons under several different take-off angles. Thereby, we deliberately break the symmetry of the setup and are able to tune sign and magnitude of the spin signals. This IPE approach with multiple photon detectors under different detection angles is advantageous with respect to typical PE setups with only one photon source at a fixed angle of incidence.

The spin- and angle-resolved IPE experiments have been performed with ROSE, our rotatable spin-polarized electron source [17]. A spin-polarized electron beam was employed to investigate the spin-dependent unoccupied electronic structure of the W(110) surface. The transversal spin polarization of the beam is rotatable. In particular, for normal electron incidence, the spin polarization can be aligned with the two mirror planes of the surface. Here, we mainly focus on two highly symmetric configurations with spin polarization either along x or y, i.e., along $\overline{\Gamma}\,\overline{N}$ or $\overline{\Gamma}\,\overline{H}$ of the surface Brillouin zone, as defined in Fig. 1(a). The emitted photons with an energy of $\hbar\omega =$ 9.9 eV are detected by several Geiger-Müller counters with different detection angles. The total-energy resolution of the IPE experiment is about 350 meV [18].

The W(110) surface was cleaned by repeated cycles of heating in an oxygen atmosphere (6×10^{-8} mbar to 1×10^{-8} mbar) at 1500 K and subsequent flashing to 2300 K.

––––––––––––

*Corresponding author: henry.wortelen@uni-muenster.de
†Present address: Max-Planck-Institut für chemische Physik fester Stoffe, Nöthnitzer Straße 40, 01187 Dresden, Germany.
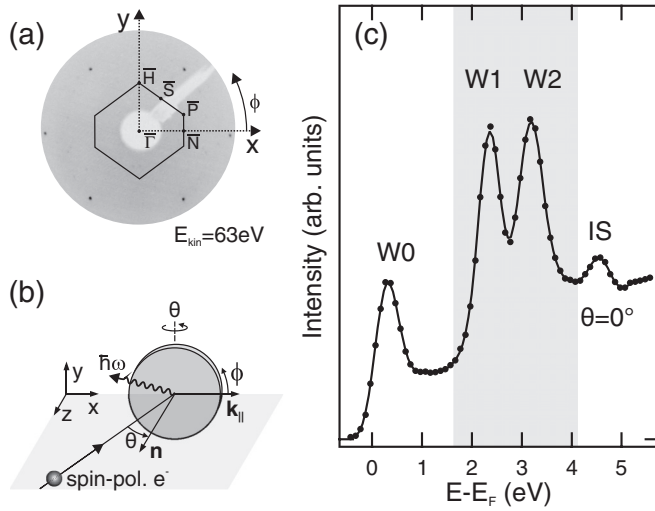
FIG. 1. (a) LEED pattern of clean W(110) for an electron energy of 63 eV. The surface Brillouin zone is shown as an overlay. The x and y axes are chosen along the $\overline{\Gamma}\,\overline{N}$ and the $\overline{\Gamma}\,\overline{H}$ symmetry lines, respectively. (b) Experimental geometry of the spin-resolved IPE experiment. Arrows of rotation denote positive direction of rotation. (c) Spin-integrated IPE spectrum (sum over all counters) for $\theta = 0°$. The gray-shaded area highlights the energy region in which W1 and W2 appear.

During the final flash, the pressure did not exceed 6×10^{-9} mbar. This cleaning procedure was successful to remove contaminants, such as carbon and oxygen, from the surface. The surface quality was confirmed by Auger electron spectra and by a sharp (1×1) low-energy-electron diffraction (LEED) pattern with low background intensity [Fig. 1(a)].

The electronic-structure calculations were performed within the framework of the local spin-density approximation to density functional theory. Our computations rely on the relativistic layer Korringa-Kohn-Rostoker method, in which spin-orbit coupling is accounted for by solving the Dirac equation [19,20]; for details, see Ref. [21]. The W(110) surface is treated as a semi-infinite system. The top layer is relaxed inward by $\Delta d = -3\%$ with respect to the bulk interlayer distance, in agreement with experiments [22,23].

From the layer-resolved Green function G_{ll} of the entire system, we calculate the spectral density $n_l(E, \boldsymbol{k}_\parallel)$ for layer l at energy E and surface-parallel wave vector $\boldsymbol{k}_\parallel$,

$$n_l(E, \boldsymbol{k}_\parallel) = -\frac{1}{\pi} \, \mathrm{Im} \, \mathrm{Tr} \, G_{ll}(E, \boldsymbol{k}_\parallel).$$

The spectral density is further decomposed with respect to angular momentum and spin projection. Spin textures are discussed by means of spin differences $n_{l\uparrow}(E, \boldsymbol{k}_\parallel) - n_{l\downarrow}(E, \boldsymbol{k}_\parallel)$, in which $\uparrow$ and $\downarrow$ refer to a specified quantization axis.

Figure 1(c) presents a spin-integrated IPE spectrum for normal electron incidence on W(110), which exhibits four distinct features. W0 just above the Fermi energy E_F is attributed to a surface state with p_z character, and IS at 4.5 eV to an image-potential-induced surface state [24,25]. W1 and W2 at 2.3 and 3.2 eV, respectively, are assigned to transitions into d states of tungsten [24].

Figure 2 reveals the spin dependence of W1 and W2. Three photon detectors with different take-off angles (α, β) have been used: ($70°, 180°$) for counter C1, ($35°, 90°$) for C2, and ($35°, 0°$) for C3, as sketched in Fig. 2(a). The polar angle α and the azimuthal angle β are defined with respect to the Cartesian coordinate system for the nonrotated sample ($\phi = 0°$), as shown in Fig. 1(b); the z axis coincides with the electron incidence direction, i.e., the surface normal.

Spectra taken with an electron spin polarization along y [Fig. 2(b)] show a remarkable result. While the spin asymmetry of W2 is zero for all counters, it exhibits values larger than 30 % for W1: positive for C1, zero for C2, and negative for C3. This result is surprising because electronic states at $\overline{\Gamma}$ have no intrinsic spin polarization due to time-reversal symmetry. Interestingly, the spin-asymmetry data with opposite sign were obtained by C1 and C3, which lie on opposite sides of the surface normal. Additional experiments with the electron spin polarization along x (by rotation of the electron source) do not lead to any spin asymmetry for all counters [Fig. 2(c)]. This reflects the twofold symmetry of the bcc(110) surface. In a control experiment, we rotated both the electron spin polarization and the sample by 90° [Fig. 2(d)]. This geometry differs from the one used for the data in Fig. 2(b) in that C1 and C3 are now in equivalent positions as C2 was before, and C2 is now in a position like C1. As a consequence, the result of C2 is expected to resemble the former result of C3, while C1 and C3 should not show any spin asymmetry. Both expectations are convincingly met by the experimental results.

Our results show that for W1, we can deliberately produce a desired spin signal from an unpolarized state, i.e., positive, zero, or negative, by carefully choosing the experimental geometry. This is demonstrated by additional results, shown in Fig. 2(e), in which the spin asymmetry of W1 is shown as a function of the azimuthal rotation angle ϕ of the sample. In this experiment, the electron spin polarization $\boldsymbol{P}$ of our ROSE was set along the y axis of the nonrotated sample. By rotating the sample, the spin signal of W1 reveals a sinusoidal dependence. Its periodicity is 180° for both C1 and C3, while it is 90°, including a sign change, for C2.

For W2, independent of the experimental geometry, no spin signal is observed, in striking contrast to W1. Two questions arise: What is the origin of this effect? What distinguishes W1 from W2?

Figure 3 presents calculations of the electronic structure of W(110) along $\overline{\Gamma}\,\overline{N}$: spectral densities $n(E, \boldsymbol{k}_\parallel)$ for the bulk [Fig. 3(a)], for the surface layer [Fig. 3(b)], and the spin difference of the spectral densities for the surface layer [Fig. 3(c)]. At the energies of W1 and W2, high spectral density is found in the bulk and at the surface. A pure surface band at lower energies with downward dispersion is attributed to W0.

To gain deeper insight into the different spin behavior of W1 and W2, we analyzed their orbital and symmetry characters. In Fig. 3(d), the orbital decomposition of the surface spectral density is shown for symmetries for which the density is nonzero. While W0 appears with an almost pure p_z orbital character and W2 with an almost pure d_{xz} character, W1 consists of two orbital contributions, d_{xz} and $d_{x^2-y^2}$. We can
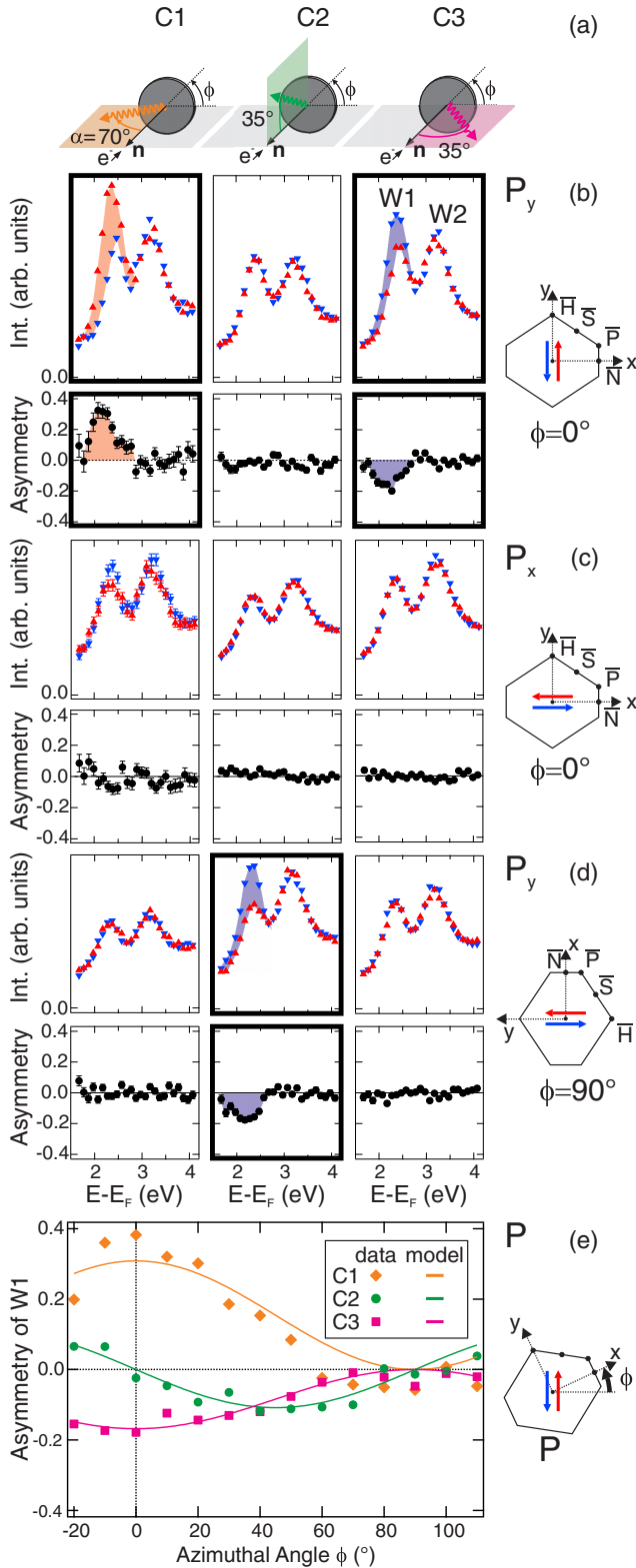
FIG. 2. (Color online) (a) Experimental geometries of counters C1, C2, and C3, with photon-detection angles specified. (b)–(d) Spin-resolved normal-incidence IPE spectra of W(110) and corresponding spin-asymmetry data for $\phi = 0°$ (sensitive to the spin-polarization components P_y and P_x) and $\phi = 90°$ (sensitive to P_y). Panels with nonzero spin asymmetry are highlighted by frames with thicker linewidth. (e) Spin asymmetry of W1 vs azimuthal angle ϕ for spin polarization **P** perpendicular to the plane of incidence.
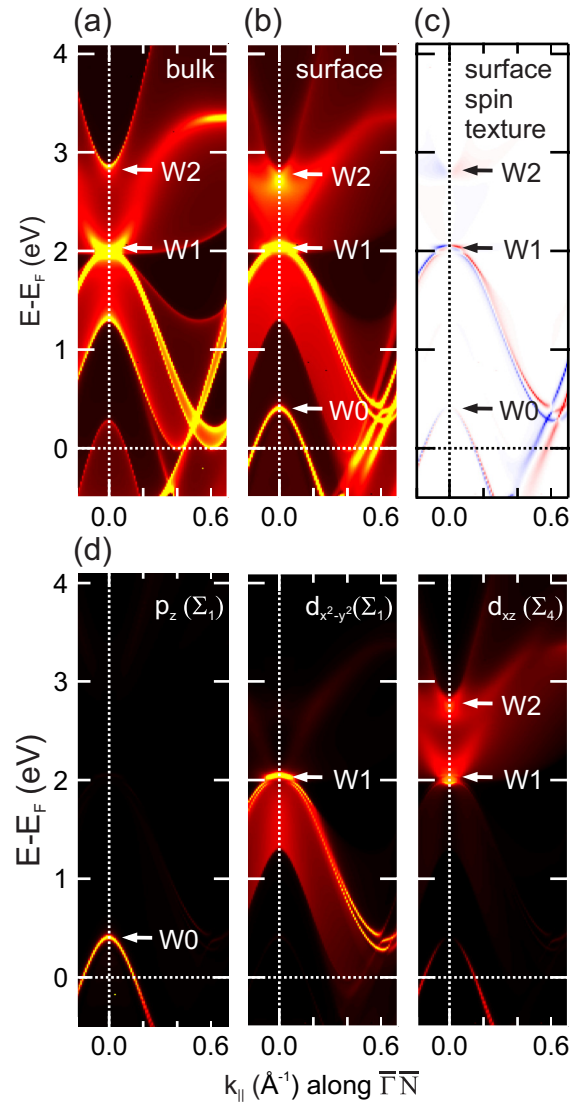
FIG. 3. (Color online) Calculated electronic structure of W(110) along $\overline{\Gamma}\,\overline{N}$. Spectral densities $n(E, \boldsymbol{k}_\parallel)$ (a) for a bulk layer and (b) for the topmost surface layer, sharing a common color scale (dark is small values and bright is large values). (c) Spin difference $n_\uparrow(E, \boldsymbol{k}_\parallel) - n_\downarrow(E, \boldsymbol{k}_\parallel)$ of the spin-projected surface spectral density, illustrated in red (blue) where spin-up (spin-down) intensity prevails (white denotes zero spin difference). (d) Orbital decomposition of the spectral density (surface and subsurface layer) with assigned symmetry representation.

assign the irreducible representation of the single group C_{2v} to the orbital contributions (neglecting spin-orbit interaction) [26]: Σ_1 to W0 and W2, Σ_1 and Σ_4 to W1. This mixed symmetry character of W1 has important consequences for its spin signal.

We now discuss these findings in the framework of a group-theoretical analysis of photoemission [27]. Within this very general approach, we restrict our present analysis to dipole-transition effects for linearly polarized light and non-magnetic materials with C_{2v} symmetry. The spin asymmetries A_y (A_x) are measured for excitation by electrons with spin polarization P_y (P_x). The theoretical analysis predicts the

following: For detection of *p*-polarized light, a spin signal A_y (A_x) is only generated by a mixing of Σ_1 and Σ_4 (Σ_1 and Σ_3) symmetry, while for *s*-polarized light, no spin signal A_x, A_y is induced. By detecting unpolarized light (which is an incoherent superposition of *s*- and *p*-polarized light), the *p*-polarized part leads to a spin signal. Since W1 is a mixed state of Σ_1 and Σ_4, a spin signal is expected for A_y but not for A_x. In contrast, no spin asymmetry is produced for W2 due to its pure representation. This is exactly what is observed in Figs. 2(b)–2(d). From theory, it follows that for dominating Σ_1, the spin asymmetry A_y can be written as $A_y \propto c(\alpha)\cos\beta$, with $c(\alpha)$ being a polar-angle-dependent amplitude. In agreement with this prediction, A_y is positive for C1 ($\beta = 0°$), 0 for C2 ($\beta = 90°$), and negative for C3 ($\beta = 180°$) in Fig. 2(b). The observed spin signals, reproduced in Figs. 2(b)–2(d), are well explained by this analysis.

Next, we address the spin-asymmetry signal observed as a function of azimuth ϕ in Fig. 2(e). Due to the concomitant rotation of the photon-detection angles relative to the sample by ϕ, the above angular dependence becomes $A_y \propto c(\alpha)\cos(\beta - \phi)$. The observed spin asymmetry A is expressed as $A_x\sin\phi + A_y\cos\phi$. Since $A_x = 0$, we arrive at

$$A \propto \begin{cases} -c(\alpha)\cos^2(\phi) & \text{for C1 } (\beta = 180°) \\ c(\alpha)\cos(\phi)\cos(90° - \phi) & \text{for C2 } (\beta = 90°) \\ c(\alpha)\cos^2(\phi) & \text{for C3 } (\beta = 0°). \end{cases}$$

Note that α is not the same for all counters and, here, $c(\alpha)$ is negative. These relations reproduce the periodicity of 90° for C2 and 180° for C1 and C3; they are used to derive the sinusoidal model curves included in Fig. 2(e).

So far, we have concentrated on the unexpected spin signal at the high-symmetry point $\overline{\Gamma}$. Away from it, Rashba-type spin dependence is expected for electronic states at surfaces of high-Z materials such as tungsten. Therefore, in Fig. 4, we show spin-resolved IPE spectra for W1 and W2 for off-normal electron incidence along $\overline{\Gamma}\,\overline{N}$ ($\phi = 0°$). The spin polarization was aligned to *y*, which is the direction of the Rashba component. The data for $\theta = \pm 8°$ reveal a sizable spin asymmetry for W2 in both counters C1 and C2, which changes sign for $\theta \to -\theta$. This clear signature of a Rashba-type wave-vector-dependent spin polarization is supported by the spin difference of the surface spectral density $n_\uparrow(E, \boldsymbol{k}_\parallel) - n_\downarrow(E, \boldsymbol{k}_\parallel)$, shown in Fig. 3(c): in the energy range of W2, the spectral density reverses sign, shown as faint blue for negative *k* and faint red for positive *k*. We conclude that for W2, i.e., the state with pure symmetry, the measured spin asymmetry reflects the intrinsic spin texture of the electronic state. For W1, the calculations predict a Rashba spin splitting into two oppositely spin-polarized states. However, the splitting is too small to be resolved by our experiment. Therefore, we do not observe a spin dependence for W1 in C2. Apart from that, the strong experimental spin signal of W1 in C1 for normal electron incidence (discussed above) persists for off-normal electron incidence. It dominates any small Rashba-type spin signal, if experimentally detectable.
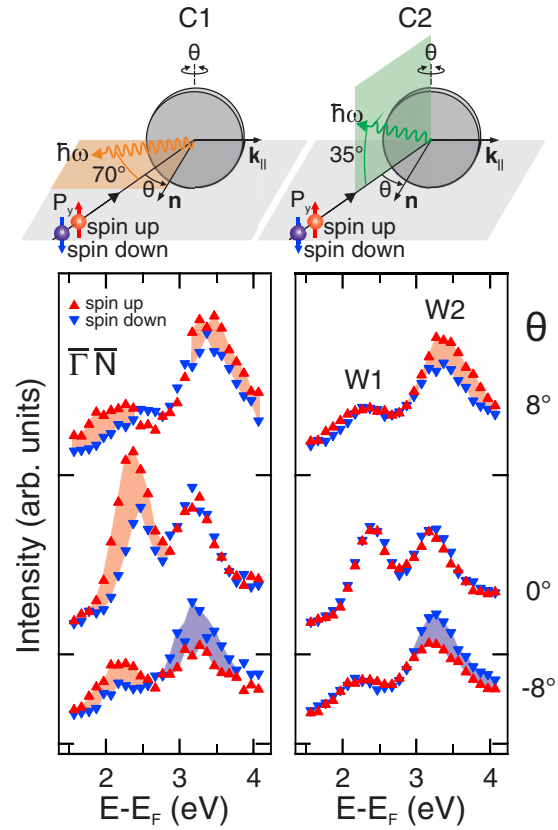
FIG. 4. (Color online) Spin-resolved IPE spectra of W(110) for various angles of electron incidence θ along $\overline{\Gamma}\,\overline{N}$ ($\phi = 0°$), sensitive to the Rashba component P_y of the spin polarization. Photons are detected by counters C1 (left) and C2 (right). For C2 (symmetric position with respect to θ), the spin-integrated spectra for $+\theta$ and $-\theta$ are equivalent.

In conclusion, we showed that the spin signals of electronic states, observed by spin-resolved (I)PE, are not only influenced by their intrinsic spin polarization but also by the choice of symmetry-breaking experimental parameters in combination with the particular symmetry characters of the involved states. In our spin- and angle-resolved IPE study for normal electron incidence on W(110), we demonstrated how the spin signal can be deliberately tuned from negative to positive values in the absence of any intrinsic spin polarization. A group-theoretical analysis of the electronic structure revealed that this appears for states with mixed symmetry but not for pure states. The latter is convincingly confirmed by simultaneous measurements on a state of pure symmetry, which shows no spin signal. Our study has general impact in two ways: (i) the need to be careful with the interpretation of spin signals, which might not be intrinsic but offer insight into the orbital characters of the involved states, and (ii) the possibility of producing spin signals tunable in both sign and magnitude from unpolarized states.

[1] M. Hoesch, M. Muntwiler, V. N. Petrov, M. Hengsberger, L. Patthey, M. Shi, M. Falub, T. Greber, and J. Osterwalder, Phys. Rev. B **69**, 241401 (2004).

[2] D. Hsieh, Y. Xia, D. Qian, L. Wray, J. H. Dil, F. Meier, J. Osterwalder, L. Patthey, J. G. Checkelsky, N. P. Ong, A. V. Fedorov, H. Lin, A. Bansil, D. Grauer, Y. S. Hor, R. J. Cava, and M. Z. Hasan, Nature (London) **460**, 1101 (2009).

[3] T. Okuda and A. Kimura, J. Phys. Soc. Jpn. **82**, 021002 (2013).

[4] S. N. P. Wissing, C. Eibl, A. Zumbülte, A. B. Schmidt, J. Braun, J. Minár, H. Ebert, and M. Donath, New J. Phys. **15**, 105001 (2013).

[5] S. D. Stolwijk, A. B. Schmidt, M. Donath, K. Sakamoto, and P. Krüger, Phys. Rev. Lett. **111**, 176402 (2013).

[6] U. Heinzmann and J. H. Dil, J. Phys.: Condens. Matter **24**, 173001 (2012).

[7] J. Osterwalder, J. Phys.: Condens. Matter **24**, 171001 (2012).

[8] C. Jozwiak, C.-H. Park, K. Gotlieb, C. Hwang, D.-H. Lee, S. G. Louie, J. D. Denlinger, C. R. Rotundu, R. J. Birgeneau, Z. Hussain, and A. Lanzara, Nat. Phys. **9**, 293 (2013).

[9] J. Sánchez-Barriga, A. Varykhalov, J. Braun, S.-Y. Xu, N. Alidoust, O. Kornilov, J. Minár, K. Hummer, G. Springholz, G. Bauer, R. Schumann, L. V. Yashina, H. Ebert, M. Z. Hasan, and O. Rader, Phys. Rev. X **4**, 011046 (2014).

[10] S. N. P. Wissing, A. B. Schmidt, H. Mirhosseini, J. Henk, C. R. Ast, and M. Donath, Phys. Rev. Lett. **113**, 116402 (2014).

[11] B. Schmiedeskamp, N. Irmer, R. David, and U. Heinzmann, Appl. Phys. A **53**, 418 (1991).

[12] N. Irmer, R. David, B. Schmiedeskamp, and U. Heinzmann, Phys. Rev. B **45**, 3849 (1992).

[13] N. Irmer, F. Frentzen, B. Schmiedeskamp, and U. Heinzmann, Surf. Sci. **307**, 1114 (1994).

[14] K. Miyamoto, A. Kimura, K. Kuroda, T. Okuda, K. Shimada, H. Namatame, M. Taniguchi, and M. Donath, Phys. Rev. Lett. **108**, 066808 (2012).

[15] K. Miyamoto, A. Kimura, T. Okuda, K. Shimada, H. Iwasawa, H. Hayashi, H. Namatame, M. Taniguchi, and M. Donath, Phys. Rev. B **86**, 161411 (2012).

[16] E. Rotenberg and S. D. Kevan, Phys. Rev. Lett. **80**, 2905 (1998).

[17] S. D. Stolwijk, H. Wortelen, A. B. Schmidt, and M. Donath, Rev. Sci. Instrum. **85**, 013306 (2014).

[18] M. Budke, T. Allmers, M. Donath, and G. Rangelov, Rev. Sci. Instrum. **78**, 113909 (2007).

[19] J. Henk, in *Handbook of Thin Film Materials*, edited by H. S. Nalwa (Academic Press, San Diego, 2002), Vol. 2, Chap. 10, p. 479.

[20] *Electron Scattering in Solid Matter*, edited by J. Zabloudil, R. Hammerling, L. Szunyogh, and P. Weinberger (Springer, Berlin, 2005).

[21] F. Giebels, H. Gollisch, and R. Feder, Phys. Rev. B **87**, 035124 (2013).

[22] M. Arnold, G. Hupfauer, P. Bayer, L. Hammer, K. Heinz, B. Kohler, and M. Scheffler, Surf. Sci. **382**, 288 (1997).

[23] G. Teeter, J. L. Erskine, F. Shi, and M. A. Van Hove, Phys. Rev. B **60**, 1975 (1999).

[24] D. Li, P. A. Dowben, J. E. Ortega, and F. J. Himpsel, Phys. Rev. B **47**, 12895 (1993).

[25] U. Thomann, C. Reuß, T. Fauster, F. Passek, and M. Donath, Phys. Rev. B **61**, 16163 (2000).

[26] Note that spin-orbit coupling results in a single irreducible representation (Σ^5) of the double group.

[27] J. Henk, T. Scheunemann, S. V. Halilov, and R. Feder, J. Phys.: Condens. Matter **8**, 47 (1996).